



# Heterogeneous Axonal Delay Improves the Spiking Activity Propagation on a Toroidal Network

Marcello Salustri<sup>1</sup> · Ruggero Micheletto<sup>1</sup>

Received: 3 December 2021 / Accepted: 26 May 2022

© The Author(s), under exclusive licence to Springer Science+Business Media, LLC, part of Springer Nature 2022

## Abstract

Several studies have looked into how noise affects neural networks and actual brains as evidenced by transcranial random noise stimulation, which improves cognitive performance. This research aims to broaden this understanding by concentrating on the network structural heterogeneity realized by adding noise to a neural model network's axonal propagation delay. We utilized the pyNEST neural network simulator to model a network of 400 artificial Izhikevich neurons connected by a folded von Neumann neighborhood to form a toroidal shape where axonal propagation noise simulates a variable spatial spacing between neurons. In this network only one neuron is regularly spiking at first because it is specifically stimulated by a 10mA external current, while all the other neurons have no external input and are stimulated solely by the activity of their neighbors. The forward propagation of the spiking wave from the original neuron to its neighbors, and then to distant nodes on the toroidal network, was investigated. For each simulation, we recorded the activity of all the network changing several parameters to verify differences of spike activity in different positions on the torus. By manipulating heterogeneity, we discovered that adding noise helps the signal reach distant neurons in 20% less time, compared to when there is no heterogeneity. We demonstrated for the first time that structural heterogeneity in a neural network can favor the propagation of spiking waves. This result is in line with other findings that suggest that a certain level of noise is good for the brain, extending this concept to the network physical structure.

**Keywords** Noise delay · Spike · Stochastic resonance

## Introduction

Modern neuroscience copes with the considerable development of mathematical models describing the biological functioning of dynamical systems resembling the brain. To the large amount of brain-related data accumulated over time, there has been a proportional engagement in mathematical computing simulation to repeat and match the experimental results [1]. Furthermore, the counterintuitive effect of stochastic resonance plays a role in understanding how noise improves the performance of a system instead of reducing it [2].

In a larger perspective, the brain is a complex system whose signals transmissions take place in a noisy heterogeneous environment [3]. Several studies show how the presence of stochastic resonance provokes substantial improvements in signal detection [4]. In this paper, hence, we want to contribute to this field, studying the spiking activity propagation in a model network and finding a simple mathematical model explaining the mechanism for which the presence of heterogeneity [5] can improve the propagation of a signal within neurons. Noticeable examples are studies on transcranial random noise stimulation (tRNS), where subjects are stimulated by large electrodes with weak random electric stimuli that actually improve their different motor, sensory, and even cognitive tasks [6].

In this paper, we focus on another type of noise: the heterogeneity of inter-neuronal distance. In a real brain, neurons are not placed in a regular lattice, like in a crystalline structure. Instead their position is affected by a certain degree of randomness. Since in a model network, the distance between neurons is represented by the propagation delay, in this study

---

Supported by the Yokohama City University

---

✉ Ruggero Micheletto  
ruggero@yokohama-cu.ac.jp

<sup>1</sup> Graduate School of Nanobioscience, Cognitive Informatics Laboratory, Yokohama City University, 22-2 Seto, Kanazawa-ku 236-0027, Japan

we identify how the increasing of noise in axonal propagation time decreases the time delay of signal transmission through a simple network model of 400 neurons. Particularly, using an Izhikevich neuron model implemented on a toroidal framed network [7, 8], we investigate the different time delays of a signal traveling across the network while the system is undertaken to different heterogeneity levels through axonal delay manipulation. The heterogeneity has been implemented by using a uniformly distributed noise parameter. Neurons in the brain deal with information in confined areas, which generally are named and classified depending on their function. These areas, however, do not have defined ends or borders. In this sense, the choice of a torus instead of a confined layer or plane is natural because of its border-less nature. The utilization of toroidal topology in previous studies [9], together with the mathematical topological nature of the torus, which we might want to exploit for future research, led us to frame our network in the toroidal shape.

We find that the increase of axonal delay noise in the network corresponds to a decrease in the total propagation time of the signal from an input defined as *initiator*  $n_{in}$ , to an arbitrary test neuron called *output*  $n_o$ . Communication of neurons takes place through action potentials (spikes), which travel to neighbors neurons inducing other spikes. Overall this creates a wave of spikes that propagates along the network. The Hodgkin–Huxley model, introduced in 1952 and awarded with Nobel Prize in 1963, mathematically describes all the plausible action potential patterns properties of biological membranes with a large set of nonlinear differential equations [10].

Over the years, the models have been extensively analyzed for developing methods that can be used for more complex systems. An extraordinary compendium of the Hodgkin–Huxley model was presented by Eugene M. Izhikevich [11], who enhanced a model that accurately resembles the spiking and bursting behavior of cortical neurons, combining the biological outcomes of their model and the mathematical interpretation of integrate-and-fire neurons with a two-dimensional system of ordinary differential equations. Implemented by a PC program, Izhikevich could reproduce around twenty different responses which characterize real neurons spiking behavior.

As mentioned above, our model network lies on a toroidal structure to emulate confined neuronal domains. Moreover, the symmetric properties of this topology give us the advantage to have always four neighbors for each node and that makes the network a perfect n-dimensional grid.

Specifically, each node is connected to its 4 nearest neighbors and corresponding nodes on opposite edges are connected in a cyclic fashion. The communication of each node can take place in 4 directions, +x or east, -x or west, +y or north, and -y or south. A torus network can be defined as a

graph  $G = (N, C)$ , where  $N(G)$  and  $C(G)$  are, respectively, the nodes and connections of  $G$  [12]. The total nodes of the 2D torus are  $n^2$ , and the two-dimensional torus structure leads naturally to a von Neumann-shaped neighborhood [13], used to define a set of cells surrounding a given cell provided with four inputs.

We initiate the simulation by choosing a neuron (corresponding to a node in our toroidal network) that acts as a stimulus and that we name “initiator.” This is connected to a constant external current of  $I = 10mA$  to induce it to spike regularly for the total duration of the simulation (in most of our tests 1000 milliseconds). Each single node is conceived to possess an intrinsic axonal delay  $d = cd + \delta$ , where  $cd$  is called from now on “central delay” and  $\delta = nd \cdot \alpha$ . The parameter  $nd$  is called “noise delay” whereas  $\alpha = [(2x) - 1]$ ; ( $0 \leq x \leq 1$ ) is a random variable with uniform distribution used to implement the axonal propagation delay heterogeneity. We, hence, analyze the propagation of the signal within the network up to the chosen output. To gather more interesting data, we chose the two input-output neurons to have the maximum distance between them in our structure.

Given the symmetric toroidal shape of the network and considering the model to be framed over a 20×20 grid of 400 neurons, the maximum distance from two neurons is a Manhattan distance of 20, to which corresponds 10 nodes along the diagonal [14].

At the beginning of the simulation, only the initiator neuron is spiking, then the spike activity propagates up to a far away test neuron that we name the “output” node. The simulation calculates the time it takes for the first spike to reach the chosen output node. We run several simulations, in each of which we increase the noise delay using the randomly uniform distribution of the parameter  $x$  of  $\alpha$ . Since the dis-homogeneity is random and uniform, we should not expect any advantage due to the noise, instead, we will prove that it favors a faster propagation of spiking activity and we will give a simple theoretical framework to understand why.

## Methods

To implement our simulation, we used Python and the NEST library version 2.2 [15], which enabled us to portray a neural-dynamic experiment by creating and connecting neurons to simulate a spiking network in continuous time. With the NEST library, we were able to implement specific functions to large sets of nodes whose connections have a configurable delay/weight as well as parameters and state variables. The library functionality to implement loops and integrate the Izhikevich differential equations, simplifies the process of software development [16].

In our structure, we used the neuron model developed by Eugene Izhikevich. Among several models for studying spiking neural networks (SNN), we use the model proposed by Izhikevich because of its high plausible biological dynamics, fundamental to reproducing well the non-linear phenomena dynamics of the neural network. Without realistic neuronal dynamics, we will not be able to explain the faster spiking activity propagation caused by the increased spatial heterogeneity in the network. Furthermore, by properly setting a few parameters, the Izhikevich neuron model reproduces most of all spiking activities, offering a solid accuracy to reproduce spike patterns [17]. Concerning the propagation delay between neurons, in NEST, it is implemented by a pipeline/buffer procedure. At each time step, a Runge-Kutta engine processes the Izhikevich model differential equations in which the input of the presynaptic neuron is taken into account by a weighted sum (the weights represent the synaptic connection strength parameter). However, if a neuron is delayed by a certain time, its signal circulates in a memory register, a *pipe*, long as the delay is measured in time steps number. In other words, at each time step, the presynaptic membrane potential is inserted at the beginning of the pipe, whereas the last element is fed to the Izhikevich differential equation. Since the pipe is rolled one step forward at each time step, and because it is as long as the delay, this method implements the time delay between presynaptic and post-synaptic neurons in a seamless manner without interfering with the theoretical models of the delays in this study.

The model describes the time evolution of the membrane potential  $v$  using a two-dimensional system of ordinary differential equations with four parameters  $a, b, c,$  and  $d$  which characterize both the spiking and the bursting behavior of the neurons [11]

$$\begin{cases} v' = 0.04v^2 + 5v + 140 - u + I \\ u' = a(bv - u) \end{cases}$$

with after the spike, a reset process is given by:

$$\text{if } v \geq 30mV \rightarrow \begin{cases} v \leftarrow c \\ u \leftarrow u + d \end{cases} \quad (1)$$

where  $v' = \frac{dv}{dt}$ , and  $u' = \frac{du}{dt}$ .

The variables  $v$  and  $u$  and the parameters  $a, b, c$  and  $d$  are all dimensionless [11],  $t$  is the time. In the mathematical model,  $v$  represents the membrane potential and  $u$  a membrane recovery variable, providing the negative feedback to  $v$ . After each spike, according to Eq. (1) the membrane voltage and the recovery variable are reset down to the parameter  $c$  and to  $u + d$ , respectively.  $I$  is the variable representing the external current stimulus, while the adjustment  $0.04v^2 + 5v + 140$  allows the membrane potential  $v$  and time  $t$  to be scaled, respectively, to  $mV$  and  $ms$ .

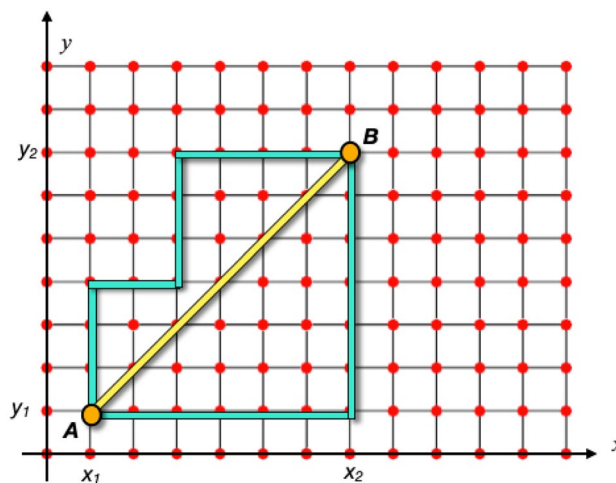


**Fig. 1** There are several shortest paths to go from **A** to **B**, but the Manhattan distance, which in this case is 12, is the same for any shortest path. Instead, in the case of Euclidean distance, there exists one and only one shortest path from **A** to **B**

The parameters  $a, b, c$  and  $d$ , according to their values, enable the equation to depict various firing patterns model. In particular:

- $a : (0.02 \text{ msec}^{-1})$  represents the recovery time for  $u$ ; to an increment of  $a$ , resulting in a quicker recovery for  $u$ .
- $b : (0.20)$ [dimensionless] underlines the strength of  $u$  to the sub-threshold fluctuations of the membrane potential  $v$ . An increment of  $b$  is translated into a stronger interrelation between  $u$  and  $v$ , meaning possible sub-threshold oscillations and low-threshold spiking dynamics.
- $c : (-65mV)$  represents the after-spike reset value of the membrane potential  $v$ .
- $d : (6mV)$  describes the after-spike reset of the recovery variable  $u$ .

The model of Izhikevich empowers us to define each neuron with an accurate and biologically feasible mathematical structure, leaving us with the only need to establish a plausible connection structure for each node/neuron of our network.

A reasonable choice to design the dynamic network, find its natural place in the two-dimensional lattice von Neumann neighborhood (4-neighborhood model as in Fig. 2), where each cell is connected with its four adjacent cells located on its north, south, east and western position [13]. In machine learning, the Manhattan distance (or taxicab geometry) is used to calculate the distance (or “closeness”) between two points/nodes. Contrary to the Euclidean distance, there may be several different paths with the same Manhattan distance between two points, as shown in Fig. 1.

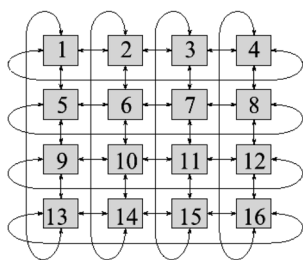


**Fig. 2** Toroidal network of 16 neurons plotted in  $4 \times 4$  square matrices. To create a biologically plausible continuous system, which is to avoid the presence of boundaries or borders in the structure, the first row is connected to the last row and the first column to the last one

Once we have defined the new metric, we generate a two-dimension matrix of 400 neurons connected according to the von Neumann neighborhood model and consider the first row to be up-connected with the last row (and vice-versa), and the first column to be left-arrow connected with the last column and vice-versa (see Fig. 2 for a schematic example of the structure). In this way, by theoretically bending the edges, we reshape the two-dimension matrix in a tree-dimension torus, on the surface of which lays our dynamic network that represents a model of a neural aggregate where information is confined into. This leads to a resembling affinity with the toroidal neural networks (TNN) [18], defined by 2D toroidal topology. The toroidal structure addresses the study to several appealing geometric interpretations.

For instance, as we can see in Fig. 3, the development of spike rate on a toroidal surface tends to approach the geodesic line, a locally length-minimizing curve. From a topological perspective, the torus shows important homeomorphic properties, empowering the research to deepen further studies in computational topology for improving the understanding of brain functionality [19, 20].

Once we framed the network in a toroidal model and defined the neurons according to Izhikevich’s archetype, we run the simulations. In the first part of the program, we built a matrix whose nodes represent the neurons, connected in a pattern to form the grid of toroidal structure with 400 neurons ( $20 \times 20$  arrays). To maintain the system in its simplest form all neurons are considered identical, there are no inhibitory synapses and no thalamic currents. We want only to focus on the effect of dis-uniform axonal propagation delay [21], so we study the model at its prime conditions. In this, we considered RS (regular spiking) neurons, cause they address the most typical neuron class in the cortex.

We use the following terminology to identify the delay and strength connection for a neuron. Each of them is here characterized by its synaptic strength connection  $w$ , which is constant all along with the network and will not be considered in our calculation.

As introduced above, the intrinsic axonal delay for each neuron is, in general, defined by the variables  $d = cd + \delta$  where  $cd$  represents the time it takes for the spike to propagate along the axon and  $\delta$  is a random variation around this value. We have two main loops. The external one runs the integer  $j$  that varies the neuron *central delay*  $cd$ , whereas the internal loop runs  $i$  that changes its stochastic *noise delay* part  $\delta$ . We initially assigned a value to the variable  $ns$  (for noise steps) and  $(cd)_{max}$ , representing respectfully the number of  $i$ -loop and  $j$ -loop such that:

$$1 \leq i \leq ns, \text{ and } 1 \leq j \leq (cd)_{max}, i, j \in \mathbb{N}$$

When  $i$  reaches  $ns$ , after  $ns$   $i$ -loops,  $j$  increases of 1. For simplicity, we consider the value of the  $j$ -th central delay  $(cd)_j$  to be equal to  $j$ , so it assumes the integers values  $(1, 2, 3, 4, \dots, (cd)_{max})$ . Therefore, this structure realizes a heterogeneous intrinsic delay  $d_{i,j}$  for each neuron. The variable parameter is formulated as follows:

$$d_{i,j} = (cd)_j + \delta_{i,j} = (cd)_j + (nd)_{i,j} \alpha_{i,j} \tag{2}$$

where

- $\alpha_{i,j} = \lfloor (2x_{i,j}) - 1 \rfloor$
- $(cd)_j = \text{central delay}; 1 \leq (cd)_j \leq (cd)_{max}, j \in \mathbb{N}$
- $\delta_{i,j} = (nd)_{i,j} \cdot \alpha_{i,j}; (\delta_{i,j} \leq (cd)_j)$
- for each  $j$ :  $(nd)_{i,j} = i \frac{(cd)_j}{ns}, 1 \leq i \leq ns, i \in \mathbb{N}$  where  $0 \leq x_{i,j} \leq 1$  is an aleatory variable with uniform distribution assigned to each neuron at the  $i$ -loop and  $j$ -loop. In this way  $\alpha_{i,j}$  is always within the  $-1, +1$  interval.

The simulation starts with  $j=1$  ( $cd=1$ ) which, at each  $i$ -loop, assigns to each neuron an intrinsic delay  $d_{i,j}$ , whose value, according to Eq. (2), ranges as follows:

$$(cd)_j - (nd)_{i,j} \leq d_{i,j} \leq (cd)_j + (nd)_{i,j}$$

For any single  $(cd)_j$ , we run  $ns$  number of  $i$ -loops ( $ns$ -simulations) and get the value for  $(nd)_{i,j}$  as follows:

$$(nd)_{i,j} = i \frac{(cd)_j}{ns}, 1 \leq i \leq ns, i \in \mathbb{N} \tag{3}$$

This framework realizes a network of 200 neurons, each of them having a different (heterogeneous) intrinsic axonal delay  $d_{i,j}$ . In the whole network, only the special neuron  $n_{in}$  is stimulated by an external current  $I = 10\text{mA}$ . Once this starts to spike regularly, its activity propagates to its neighbors with a certain delay. Then its neighbors once activated, will transmit their activity to others and so on. To measure the spike activity propagation speed between two defined neurons, a neuron distant from  $n_{in}$  is used to *test* the arrival time of the spike information coming from  $n_{in}$  itself. This neuron

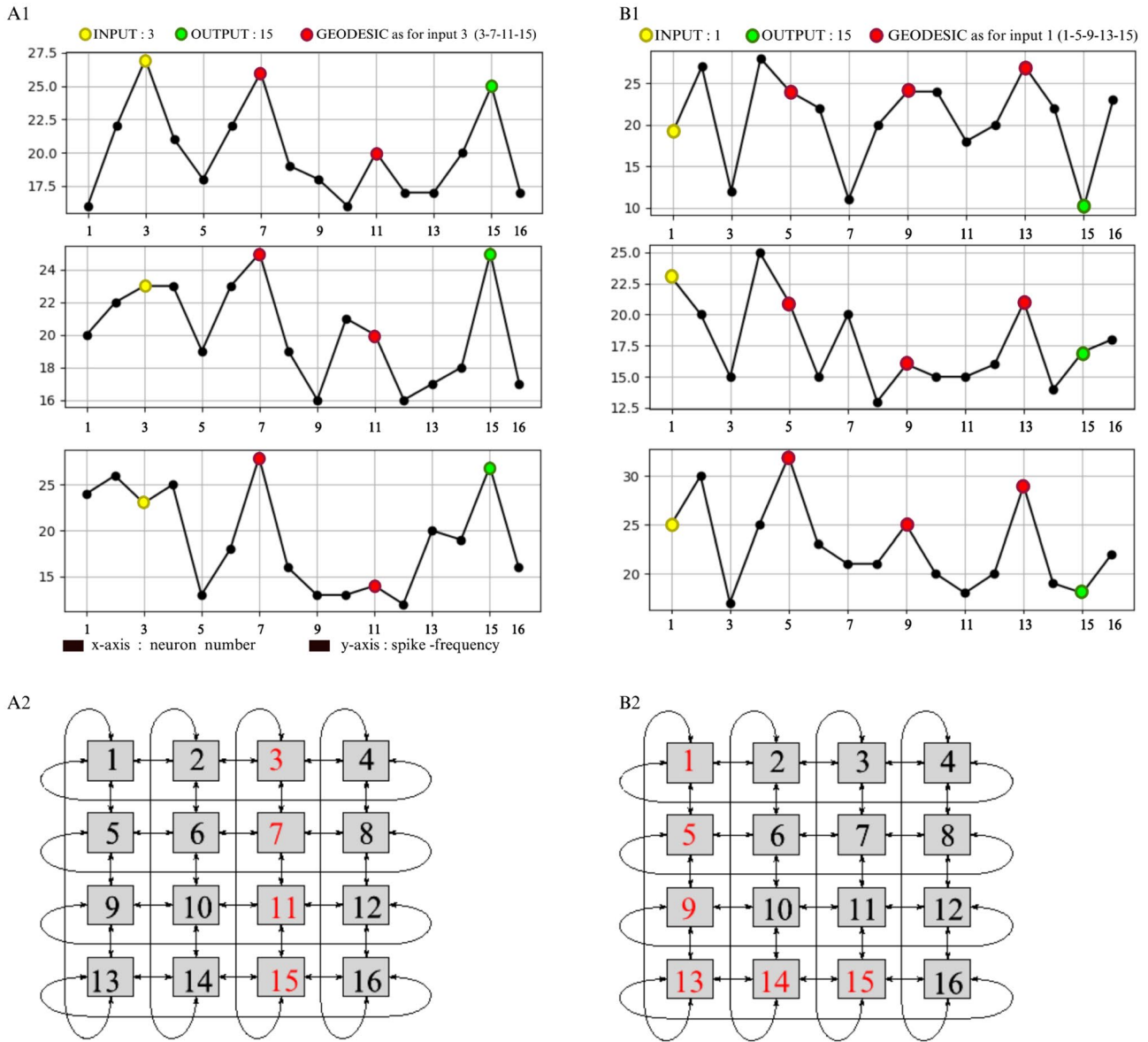


**Fig. 3** In **A1** and **B1** we run three simulations on the toroidal network of Fig. 2. Neuron 3 is considered the input of the network, being the only one connected to the external input and to initially spike. The three plots in **A1** show the spike rate calculated in three different simulations of 1000 mseconds. In **B1** other three simulations are shown, but this time the input neuron is in position 1. On **B1** the path 1-5-9-13-14-15 shows higher spiking frequency on the nodes 1-5-9-13, compared to paths with the same Manhattan distance as, for instance,

the sequences 1-2-3-7-11-15 or 1-2-6-10-11-15. In **A1**, if we don't consider the direct connection 3 to 15, the shortest path from input(3) to output(15) is 3 steps. Nevertheless, a high spike frequency tends to lay on the path 3-7-11-15. Alternative paths with the same Manhattan distance are 3-2-14-15 and 3-4-16-15. In the three-dimensional torus, if we consider the Euclidean distance, the sequences in red in **A2** and **B2** (1-5-9-13) tend to lay on the longitudinal geodesic, which, eventually, would be interesting in terms of optimization of a network

is indicated with  $n_o$ . The subscripts *in* and *o* stand loosely for *input* or *initiator* and *output*, respectively.

Consequently, we define:

- $f_{out}^{ij}$  as the time of the first spike of  $n_o$ .
- $f_{in}^{ij}$  as the time of the first spike of  $n_{in}$ .

Accordingly, we can infer the *spike propagation delay* from  $n_{in}$  to  $n_o$  as:

$$\Delta f_g^{ij} = f_{out}^{ij} - f_{in}^{ij} \tag{4}$$



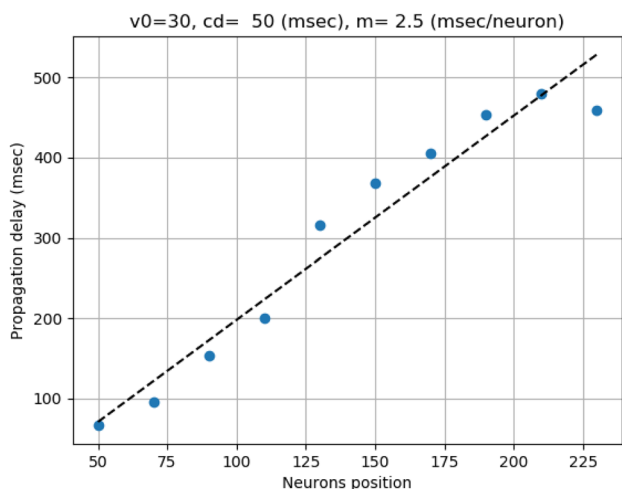


**Fig. 4** The spike activity propagation delay on the torus. Here the first spike happens at time  $t = 0$  at the node located at index 30, the delay is calculated when the neuron at the node in the position indicated on the horizontal axis has its first spike. The tested neurons are those located at the geodesic of the toroidal grid. There is a linear dependence between nodes distances and propagation  $m = 2.5$  msec/neuron represents the inclination of the linear regression. In these tests the intrinsic delay and delay heterogeneity are kept constant at  $cd = 50$  msec and  $\delta = 12.5$  msec, respectively

where  $g$  represents the minimum number of steps from  $n_i$  to reach  $n_o$ , that is, the minimum Manhattan distance [18] between the two neurons.

For each  $i$ , therefore, we identify a specific  $\Delta f_g^{i,j}$ , and for a whole  $i$ -loop we gather  $ns$  values for it.

All the  $\Delta f_g^{i,j}$  of one  $i$ -loop have the same central delay  $(cd)_j = j$ . When  $i$  reaches  $ns$ , the central delay  $(cd)_j$  is incremented of 1 and starts another cycle of  $i$ -loops.

As already stated, when  $j$  reaches  $(cd)_{max}$ , the simulation stops, leaving us with  $ns \times (cd)_{max}$  values of  $\Delta f_g^{i,j}$  to be analyzed.

From the data, we can infer if and how the increase of noise delay  $(nd)_{i,j}$  has affected the transmission of the spike signal. More accurately, we want to ascertain if the increase of  $(nd)_{i,j}$  decreases  $\Delta f_g^{i,j}$ . For this purpose, in the next section we consider to compare the regression line for each  $i$ -loop.

## Results and Discussion

To explain the effect of noise on the delay, firstly we observe how the spike activity propagation time evolves along with the network when it has a constant value of delay heterogeneity. In Fig. 4, with we pose  $(cd) = 50msec$ , with  $(nd) = (cd)/4 = 12msec$ . Again, only neuron  $n_{in}$  is spiking initially, and in the plot we show the “time of first spike” of all other neurons. Since the spike activity is propagating from  $n_{in}$  in all directions in the network, this time of the first

spike can be also called *time of arrival* in the sense that it represents the time in which the information from  $n_{in}$  arrives at another neuron. As expected, we have a linear proportionality between the Manhattan distance between the test neuron and the initiator. In our specific case, the network is a grid of  $20 \times 20$  neurons. Thus, identifying the neurons with an index that counts each of them along the grid, and setting the initiator in the center of the second row, gives the initiator the index of 30 (20 neurons for the first row, plus 10 neurons for the middle position in the second row). With this indexing convention, we test the time of arrival of the spike-wave, for each neuron along the geodesic toward the output neuron 230 (placed as well on the geodesic line, on the central row).

As noticeable from the simulation results of Fig. 4, the propagation delay in milliseconds is growing linearly with distance as intuitively we expect.

So, considering the time of spike arrival for each neuron in the network, we could elucidate if and how noise improves the circulation of spike activity in a robust and reproducible way. In Fig. 5 are shown two maps representing the toroidal network at two different noise levels. Each block represents one of the neurons and the color represents the time of the first spike in milliseconds. Since the only neuron that is stimulated externally is the *initiator* located in position  $x = 10, y = 2$  in the grid (its index is then 30), all the neurons that are spiking, do so because of spike axonal propagation along the network. When the noise level is lower (Fig. 5A,  $nd_{i,j} = 5msec$ ) the number of neurons never reached by the spiking activity is larger (deep purple color in the map). Instead when the noise level is higher (Fig. 5B,  $nd_{i,j} = 31msec$ ), the opposite phenomena is observed. Overall speaking, this leads to conclude that increasing the noise will cause the *total propagation delay*  $d_{f_{fp}}^{i,j}$  of the network to decrease. If we consider Eq. (4), we can understand that by increasing the noise parameter  $(nd)_{i,j}$  (that is when  $i$  is big), the probability to have  $\Delta f_g^{i,j} < \Delta f_g^{e,j}$  for most simulations increases. Namely, the regression line will be negative, that is,  $m < 0$ .

To describe the effect of noise on the delay, we reckon the general equation for the regression line [22]:

$$\bar{y} = \hat{m}\bar{x} + \hat{a}$$

where

$$\hat{m} = \frac{\sum_{i=1}^n (x_i - \bar{x})(y_i - \bar{y})}{\sum_{i=1}^n (x_i - \bar{x})^2} = \frac{\sigma_{x,y}}{\sigma_x^2} \tag{5}$$

Here we introduce

- $\bar{x}$  and  $\bar{y}$  as the average of the  $x_i$  and  $y_i$ .
- $\sigma_x$  and  $\sigma_y$  as the standard deviations of  $x$  and  $y$ .

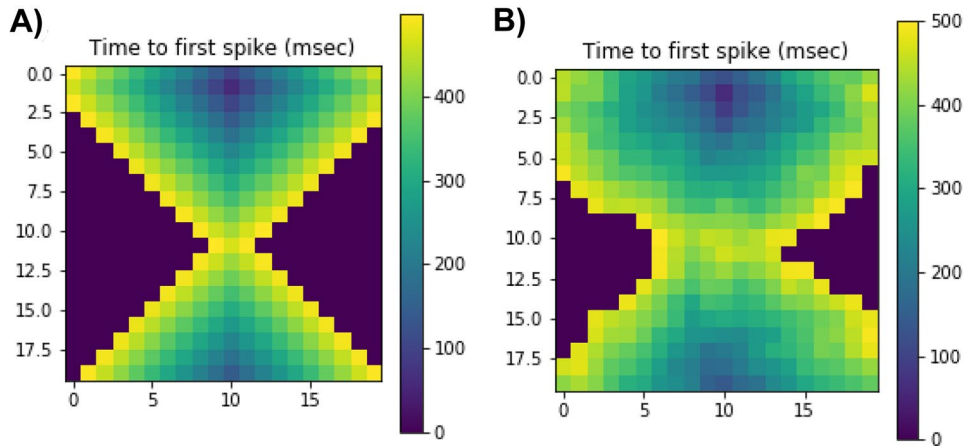


**Fig. 5** We show the spike delay for each neuron of the  $20 \times 20$  toroidal network. For each neuron in the network, we report the first spike occurrence’s time, representing the time of arrival of the spike information of the neuron that initially is spiking. This is the *initiator* neuron  $n_m$  of index 30, located in  $x = 10$  and  $y = 2$  in the map, which is spiking from  $t = 0$  due to a constant input current  $I_0 = 10mA$ . The color bar shows the time of the first spike for each neuron in milliseconds. The dark blue regions are where the neurons never spike,

i.e., the spiking activity from the *initiator*  $n_m$  doesn’t arrive in time in those locations (our test simulation is of 500msec). Noticeably, in panel 1 the noise level is small ( $nd_{i,j} = 5$  msec) a good portion of the network is never reached by the spike activity, whereas when the noise level is higher (panel 2,  $nd_{i,j} = 31$  msec) the circulation of spikes is faster with more neurons reached by the activity of the initiator

- $\sigma_x^2$  and  $\sigma_{x,y}$  as the variance and covariance.

In our model  $(x_{i,j}; y_{i,j}) = ((nd)_{i,j}; \Delta f^{i,j})$ .

We now try to give a mathematical formulation for  $m$  and prove that since from our data  $m < 0$ , then we must have, in general,  $\Delta f^{(i,j)} < \Delta f^{(e,j)}$  when  $e \leq i$ . In other words, when the noise ( $\delta$ )<sub>*i*</sub> increases, the delay  $\Delta f_g^{i,j}$  decreases. From Eq. (5), we calculate the slope for the linear regression<sup>1</sup>, where:

$$\sigma_x^2 = \frac{\sum_{i=1}^{ns} (x_i - \bar{x})(x_i - \bar{x})}{ns} \tag{6}$$

$$\sigma_{x,y} = \frac{\sum_{i=1}^{ns} (x_i - \bar{x})(y_i - \bar{y})}{ns} \tag{7}$$

our, respectively, values are:

- $x_i^j = (nd)_{i,j} = i \frac{(cd)_j}{ns}$ ;  $\bar{x} = \frac{(cd)_j(ns+1)}{2ns}$
- $y_i^j = \Delta f^{i,j}$ ;  $\bar{y} = \frac{\sum_{i=1}^{ns} \Delta f^{i,j}}{ns}$

To simplify the symbolism from now on, we reckon  $cd_j = cd$ , and  $\Delta f^{i,j} = \Delta f^i$ . We omit the index  $j$  since  $cd_j$  is constant during the calculation of a single  $m$  while only  $i$  ranges from 1 to  $ns$ . By substituting  $x_i$ ,  $\bar{x}$ ,  $y_i$ ,  $\bar{y}$  respectfully in Eqs. (6) and (7), we get:

$$\sigma_x^2 = \frac{\sum_{i=1}^{ns} (x_i - \bar{x})^2}{ns} = \frac{(cd)^2 (ns^2 - 1)}{ns^2 \cdot 12}$$

and

$$\sigma_{x,y} = \frac{(cd)}{ns^2} \left[ \sum_{i=1}^{ns} (i \Delta f^i) - \frac{(ns+1)}{2} \sum_{i=1}^{ns} \Delta f^i \right]$$

which we can write as:

$$\sigma_{x,y} = (cd)ns^2 \sum_{i=1}^{\frac{ns-1}{2}} \left| \left( i - \frac{ns+1}{2} \right) \right| (\Delta f^{(ns+1-i)} - \Delta f^i)$$

From (5), we can formulate:

$$m = \frac{\sum_{i=1}^{\frac{ns-1}{2}} \left| \left( i - \frac{ns+1}{2} \right) \right| (\Delta f^{(ns+1-i)} - \Delta f^i)}{(cd) \cdot \frac{(ns^2-1)}{12}}$$

We have  $m < 0$  only if the numerator is negative, therefore, for most of the  $\Delta f^i$ , it must follow:

$$\Delta f^{(ns+1-i)} < \Delta f^i \tag{8}$$

The Eq. (8) demonstrated how, by increasing the index  $i$  (i.e., noise), the delay of a signal is reduced compared to the preceding one. As a result, we can conclude that increasing noise reduces the delay of a signal from input to output for a fixed central delay  $(cd)_j$ .

<sup>1</sup> It is just reported a part of the demonstration.

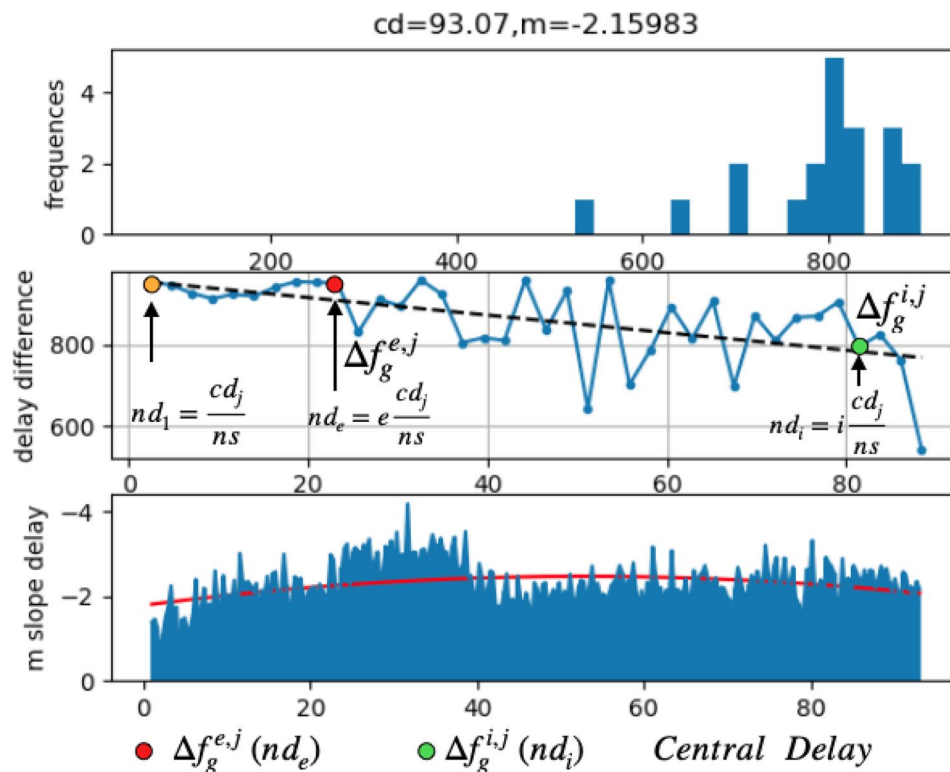


**Fig. 6** In the top panel, we plot the histogram of the time difference between the first spike of the *output* neuron  $n_o$  and the first spike of the *initiator*  $n_{in}$ . These times represent the times of arrival of the spiking activity from an *initiator* neuron placed at the position 30 to a *test* or *output* neuron placed far away in the toroidal network (in position 230). We performed 40 simulations with increased noise levels, from  $cd/40$  msec up to a maximum of  $cd = 100$  milliseconds. The resulting histogram is centered around a delay difference  $\Delta f_g^{i,j}$  of about 800 milliseconds. In the central panel, we plot the same arrival times differences in function of the noise  $(nd)_{i,j}$ . We have 40 increasing values of  $(nd)_{i,j}$  from 1 to  $(cd)_j$  ( $cd$  is fixed in these plots to  $(cd)_j = 93.07$ ). We notice that for a small value of heterogeneity  $((nd)_{i,j}$  between 0

and 23), the delay difference doesn't change much, positioning itself on values greater than 800. Eventually, by increasing the noise,  $\Delta f_g^{i,j}$  decreases accordingly, reaching values below 800 msec. The dotted line represents the linear interpolation with an inclination of  $m = -2.15$ , as indicated in the figure's title. In the bottom panel, we plot all the values of  $m$  obtained by previous simulations, where each one has a different neuronal intrinsic delay  $(cd)_j$  (ranging from 5 to 100 msec at 1 msec steps). While the top and central panel refer only to the value of  $(cd)_j = 93.07$ , the bottom panel reports all the previous values of  $m$  up to the current  $(cd)_j$ . A negative  $m$  indicates that the value of delay is decreasing

In our study, we changed the intrinsic axonal delay  $(cd)_j$  from 1 up to 100 milliseconds. For each of these values, we tested forty different levels of noises, ranging from  $(cd)_j/40$  up to  $(cd)_{max} = 100$  msec. The top panels of Figs. 6 and 7 show the distribution of the spike arrival times in the *output* neuron  $n_o$ . In Fig. 6, the central intrinsic delay is large, 93 msec, so only 20 arrival times are reported. Our simulation lasts 1000 msec, and depending on the variability of the stochastic  $\delta_{ij}$  factor, in some cases, the neuron  $n_o$  is never triggered to spike (the spike information from  $n_{in}$  doesn't arrive in time). Instead, as in Fig. 7, the histogram is complete when the central delay ranges around 31 msec. It has 40 arrival times, with the distribution concentrated on a shorter delay (approximately 350 msec). The central panel of these figures shows the time of the first spike at  $n_o$  for increasing  $(nd)_{i,j}$ . The dark dotted line in the linear regression depicts

the significant characteristic of how such time decreases as the noise level rises. Interestingly, examining the bottom panel of both figures, the slope of the regression  $m$  is always negative, with a minimum outcome around  $cd = 35$  msec (the y axis is reversed).

The bottom panel of Fig. 6 reports the value of  $m$  for each  $cd$ , from the first to the last simulation (i.e.,  $2 \leq cd \leq 93.07$ ). We were able to reproduce the minimum value of  $m$  around  $cd = 35$  msec for repeated identical simulations with different random seeds. The peak of  $m$  was always located around a global minimum between  $30 \leq cd \leq 35$ .

The slope  $m$ , which indicates how noise reduces the propagation speed within the network, remains negative in all simulations we've conducted. The fact that this occurs in a repeatable manner demonstrates the robustness of this feature in our model neural network.



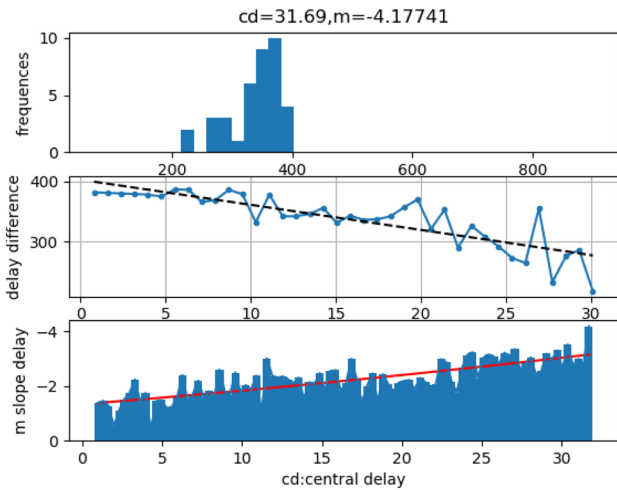


**Fig. 7** Same as Fig. 6. Precisely, we present the value of  $m$  corresponding to the global minimum for  $m = -4.17$  (in the graph, minimum appears as a maximum as the ordinate are inverted for clarity). The biggest effect of delay difference was observed in all of our testing for intrinsic delay values in the range  $31 \leq cd \leq 35$ . When the intrinsic delay is centered at 35 msec, the signal from  $n_{in}$  propagates faster

### Model

We'll now try to give a theoretical interpretation of the negativity of  $m$ .

To do so, we must investigate the neuron's dynamic system characteristics, which necessitates an understanding of

the membrane potential/recovery system's phase portrait. Conditions such as the equilibrium, limit circle, attractor [11], and other characteristics in the phase space help to clarify the spiking behavior from a dynamical system point of view.

We analyze here two phases, starting with the situation of a neuron in an equilibrium state, whose membrane potential is resting [23].

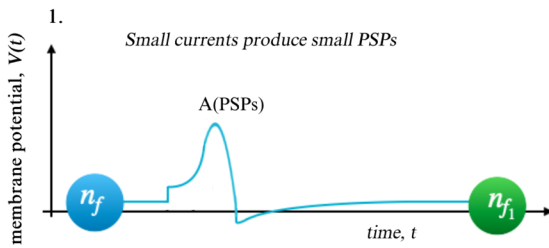
In Fig. 8(1), input currents produce a small amount of presynaptic potential (PSP) [24], in the phase diagram of Fig. 8(2) its membrane potential moves a bit around the equilibrium (black spot, *attractor-resting potential*) and, after few milliseconds, it will go back to its resting position.

Instead, in Fig. 8 panel 3, we show the effect of two presynaptic stimuli. A little signal PSPs (A) causes a slight change in the equilibrium, whereas a bigger signal PSPs (B) causes the neuron's intrinsic dynamics to spike after a short time. The period between the arrival of the stimulus and the realization of the spike is referred to as *process time*.

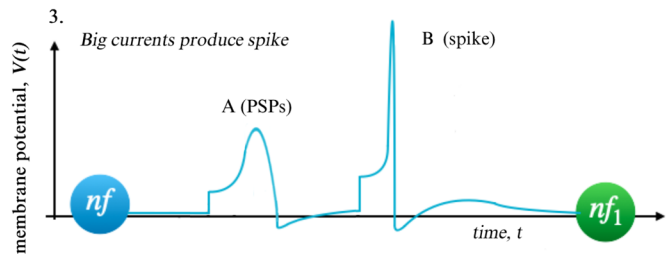
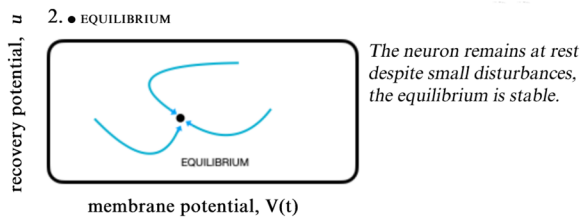
Now we'll look at what happens when a PSP signal A reaches a postsynaptic neuron while that same neuron is still firing as a result of a prior PSP signal B. Consider the case where a spike leaves a neuron  $n_f$  and travels in the direction of neuron  $n_{f1}$ .

Firstly we define:

- Process time  $\tau_f^{ij}$ : that represent the time for neuron  $n_f$  to process a presynaptic spike and deliver its own postsyn-



PSPs signal A from  $n_f$  to  $n_{f1}$



PSPs signal A from  $n_f$  to  $n_{f1}$  stimulates the signal B to spike.

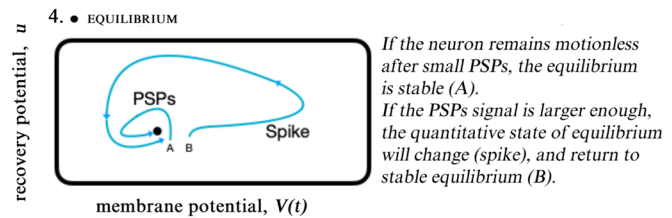


**Fig. 8** Panels 1 and 2: a stable equilibrium. A small presynaptic signal (PSP) goes from neuron  $n_f$  to  $n_{f1}$ . The membrane potential will fluctuate around the equilibrium point before returning to its resting state (black dot, the equilibrium point). Panels 3 and 4 depict the responses of two different presynaptic stimuli. The small PSP (A)

doesn't induce a spike, whereas a bigger PSP (B) does. The time it takes for the neuron to achieve a spike following the PSP is referred to as *process time*, and it is measured in milliseconds as in the Izhikevich regular spiking neurons employed in our model

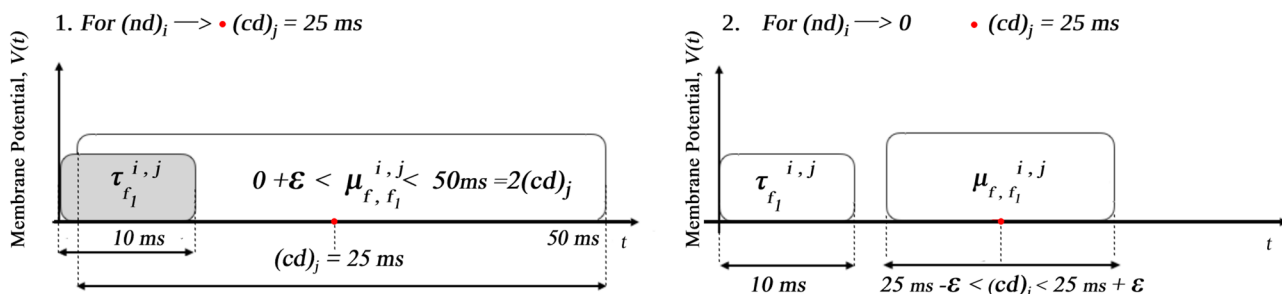


**Fig. 9** A sketch representing how the variability of the axonal delay influences the overall spike activity propagation along with the network. Two cases are shown: in panel **1**, the variability of the axonal transmission  $\mu_{f,f_p}^{i,j}$  is wide (from zero to 50ms in this example where the central value of the delay is 25ms). Since this value can become smaller than the processing time  $\tau_{f_p}^{i,j}$ , this will positively influence the

phase space of the neuron’s dynamic, resulting in a faster postsynaptic response. In panel **2** it is shown the opposite situation in which the variability of the axonal delay is smaller and never realizes this condition. Since a longer than average,  $\mu_{f,f_p}^{i,j}$  doesn’t increase postsynaptic process times, whereas a shorter than average does, this indicates how a degree of randomness helps the overall circulation of spike activity on the toroidal network

aptic spike, the two indexes  $i$  and  $j$  represents the current central delay  $(cd)_j$  and noise delay  $(nd)_{i,j}$ .

- Axonal transmission delay  $\mu_{f,f_p}^{i,j}$ : the time for a spike to go from neuron  $n_f$  to one of its four adjacent neuron  $n_{fp,(p=1,2,3,4)}$ , explicated as:

$$\mu_{f,f_p}^{i,j} = (cd)_j + nd_{f,f_p}^{i,j} = (cd)_j + i \frac{(cd)_j}{ns} \cdot (2x_{f,f_p}^{i,j} - 1) \quad (9)$$

- Total transmission delay  $d_{f,f_p}^{i,j}$ :

$$d_{f,f_p}^{i,j} = \mu_{f,f_p}^{i,j} + \tau_f^{i,j} \quad (10)$$

We need four indexes because in our model, each changing of the noise delay  $(nd)_{i,j}$ , corresponds to an  $i$ -simulation, which associates to any single neuron. The random variable  $0 \leq x^{f,f_p} \leq 1$ , characterizes the delay transmission from  $n_f$  to  $n_{fp}$ , and a process time  $\tau_f^{i,j}$ . Therefore, each  $i$ -simulation defines  $d_{f,f_p}^{i,j}$ .

Once everything is in place, the network operates as expected: a spike reaches a specific input neuron, say  $n_f$ . After a process time  $\tau_{n_f}$ , it departs  $n_f$  and reaches four adjacent neurons  $n_{fp,(p=1,2,3,4)}$  with four different axonal transmission delays  $\mu_{f,f_p}^{i,j}$  defined in Eq. (9).

Assume that some additional earlier signals  $A'$  and  $B'$ , respectively, excite the presynaptic neuron  $f$  and the postsynaptic neuron  $f_p$  at the same time (notice that the simultaneous stimulation of  $f$  and  $f_p$  has been chosen for clarity, the actual interval between the two stimuli  $A'$  and  $B'$  is arbitrary, and will not influence our general conclusion). We now want to focus on the case when :

$$\mu_{f,f_p}^{i,j} < \tau_{f_p}^{i,j} \quad (11)$$

According to Eq. (11), the spike produced by  $n_f$  will reach  $n_{f_1}$  soon, while the postsynaptic is still processing  $B'$ . The summation of these two membrane potentials, like in the phase diagram of Fig. 8(4), will push the differential equation solution to higher membrane potential, facilitating the spike generation thus reducing the processing time  $\tau_{f_p}^{i,j}$ .

When this event happens, the total time interval between the initial presynaptic stimulus caused by  $A'$  and the final postsynaptic spike  $d_{f,f_1}^{i,j}$ , will be lower than when the inequality Eq. (11) is not satisfied. In other words, because of the randomness factor within the axonal transmission delay  $\mu_{f,f_p}^{i,j}$ , this delay time will be randomly smaller or higher than average. However, only when this is smaller, the arrival of a second spike in the postsynaptic neuron will induce a lower process times in it. Instead in the other case, when  $\mu_{f,f_p}^{i,j}$  is higher, the process times  $\tau_{f_p}^{i,j}$  will not be affected. This asymmetry creates the effect that we observe in the simulations. The increasing degree of noise in the network increases the probability of this condition happening in multiple neurons, inducing faster spiking activity propagation and improving the overall circulation of information along with the network, see Fig. 9 for a sketch representing the phenomenon.

### Conclusions

We constructed a model network of 400 neurons placed on a 20x20 toroidal grid, neurons on the border are connected to those on the other extreme of the grid realizing the toroidal structure to emulate real brain patches where information exchange is confined on localized domains. We wanted to study the influence of structural heterogeneity in the network and see how it may help the diffusion

of information in the system. To do that, we made a single source of spikes, an initiator neuron  $n_{in}$  that is permanently connected to an external current  $I$  that makes it regularly spiking for the duration of the tests. The spiking activity of this neuron represents the information and it is transmitted to the adjacent nodes on the grid, distributed accordingly to a von Neumann neighborhood.

Our study shows that in this simplified model network, the time it takes for the first spike from the *initiator* neuron  $n_{in}$  to reach and induce spiking to distant neurons is decreasing with the increased heterogeneity in the axonal propagation delay. The heterogeneity is expressed by a noise factor in the axonal delay term, manipulating this parameter we found that noise favors a faster spread of information along with the network.

We devised a theoretical interpretation of this counterintuitive result, which is involving the nonlinear dynamical nature of the timing and propagation of neuronal spike activity. In our treatment, the presynaptic signal induces a spike with two different time delays, the first is considered a processing time that is intrinsically related to the differential equation representing the neuronal electrochemical dynamics and a transmission time that is inherent to the transfer along the axon. Our theoretical model shows that the random variations of transmission times due to the heterogeneity, favor faster processing reducing the overall spiking activity transfer. We have shown rigorously that this is caused by an increased probability for a second PSP to intervene when the neuron is still elaborating a previous one, effectively enhancing its action and accelerating the spike processing.

Since in biological reality, the axonal propagation delay is a proxy of the axon length or the inter-neuron distance, this shows that the randomness by which neurons are located in the brain could be interpreted as a strategy to improve and optimize the transmission of information in biological systems.

These results contribute to the understanding of the fundamental properties of information transfer in the brain, in particular, it gives a model for an explanation of other paradoxical phenomena in which noise appears to favor complex computational processes like for example transcranial random noise stimulation (tRNS) that has shown to be the most effective in enhancing neural excitability and improving perception and other cognitive tasks in human subjects.

## Declarations

**Ethical Approval** This article does not contain any studies with human participants performed by any of the authors.

**Conflicts of Interest** Marcello Salustri declares that he has no conflict of interest. Ruggero Micheletto declares that he has no conflict of interest.

## References

1. Winfree AT. The geometry of biological time. New York: Springer. 2001;12:2971–4. ISSN 978-1-4757-3484-3. <https://doi.org/10.1038/35065725>.
2. Shannon CE. A mathematical theory of communication. Bell Syst Tech J. 1948;27:373–423. 623–656.
3. Koch C, Laurent G. Complexity and the nervous system. Science. 1999;284:96–8. <https://doi.org/10.1126/science.284.5411.96>.
4. Stacey WC, Durand DM. Stochastic resonance improves signal detection in hippocampal cal neurons. J Neurophysiol. 2000;83(3). <https://doi.org/10.1152/jn.2000.83.3.1394>.
5. Perez-Nieves N, Leung VCH, Dragotti PL, et al. Neural heterogeneity promotes robust learning. Nat Commun. 2021;12. <https://doi.org/10.1038/s41467-021-26022-3>.
6. Moret B, Donato R, Nucci M, et al. Transcranial random noise stimulation (TRNS): a wide range of frequencies is needed for increasing cortical excitability. Sci Report. 2019;9. <https://doi.org/10.1038/s41598-019-51553-7>.
7. Faisal AA, Selen LPJ, Wolpert DM. Noise in the nervous system. Nat Rev Neurosci. 2008;9. <https://doi.org/10.1038/nrn2258>.
8. von Neumann J. Probabilistic logics and the synthesis of reliable organisms from unreliable components. Automata Studies. 1956;34:45–99.
9. Gardner RJ, Hermansen E, Pachitariu M, Burak Y, Baas N, Dunn BA, Moser M, Moser EI. Toroidal topology of population activity in grid cells. Nature. 2022;602. <https://doi.org/10.1038/s41586-021-04268-7>.
10. Schwiening CJ. A brief historical perspective: Hodgkin and Huxley. J Physiol. 2012;590(11). <https://doi.org/10.1113/jphysiol.2012.230458>.
11. Izhikevich EM. Simple model of spiking neurons. IEEE Trans Neural Netw. 2003;14(6).
12. Wu C, Li Y, Chai S. Design and simulation of a torus topology for network on chip. J Syst Eng Electron. 2008;19:694.
13. Tzedakis G, Tzamali E, Marias K, Sakkalis V. Routes to chaos induced by a discontinuous resetting process in a hybrid spiking neuron model. Cancer Informat. 2015;14. <https://doi.org/10.4137/CIN.S19343>.
14. Suwanda R, Syahputra Z, Zamzami EM. Analysis of euclidean distance and manhattan distance in the k-means algorithm for variations number of centroid k. J Phys. 2019;1566:696.
15. Eppler J, Helias M, Muller E, Diesmann M, Gewaltig M-O. Pynest: a convenient interface to the nest simulator. Front Neuroinform. 2009;2(12). ISSN 1662-5196. <https://doi.org/10.3389/neuro.11.012.2008>.
16. Gewaltig MO, Morrison A, Plesser HE. Nest by example: An introduction to the neural simulation tool nest. Computational Systems Neurobiology. 2012;533–558. [https://doi.org/10.1007/978-94-007-3858-4\\_18](https://doi.org/10.1007/978-94-007-3858-4_18).
17. Nobukawa S, Nishimura H, Yamanishi T. The importance of neighborhood scheme selection in agent-based tumor growth modeling. Sci Report 2018;8. <https://doi.org/10.1038/s41598-017-18783-z>.
18. Coli M, Palazzari P, Rughi R. The toroidal neural networks. 2000 IEEE International Symposium on Circuits and Systems (ISCAS). 2000;4:137–140 vol. 4. <https://doi.org/10.1109/ISCAS.2000.858707>.
19. Expert P, Lord LD, Kringelbach ML, Petri G. Editorial: Topological neuroscience. Network Neuroscience. 2019;3(3). [https://doi.org/10.1162/netn\\_e\\_00096](https://doi.org/10.1162/netn_e_00096).

20. Tozzi A, James FP. Towards a fourth spatial dimension of brain activity. *Cogn Neurodyn*. 2016;10(3). <https://doi.org/10.1007/s11571-016-9379-z>.
21. Madadi Asl M, Valizadeh A, Tass P. Dendritic and axonal propagation delays determine emergent structures of neuronal networks with plastic synapses. *Sci Report*. 2017;7. <https://doi.org/10.1038/srep39682>.
22. Schneider A, Hommel G, Blettner M. Linear regression analysis: part 14 of a series on evaluation of scientific publications. *Dtsch Arztebl Int*. 2010;107(44). <https://doi.org/10.3238/arztebl.2010.0776>.
23. Chrysafides SM, Bordes S, Sharma S. Physiology, resting potential. NCBI National Center for Biotechnology. 2021.
24. Aldrich SB. The use of multiple neurotransmitters at synapses. *Synaptic Transmission*. 2019;449–480. <https://doi.org/10.1016/B978-0-12-815320-8.00021-1>.

**Publisher's Note** Springer Nature remains neutral with regard to jurisdictional claims in published maps and institutional affiliations.